SUPPLEMENTARY MATERIAL

Selective electrochemical oxidation of organic compounds in a mass transfer-enhanced electrochemical flow reactor (e^-NETmix)

Clarissa H. Rosa [a,b,c,1], Daniela F.S. Morais [b,c,1], Gilber R. Rosa [a], João H.Z. dos Santos [d], José Carlos B. Lopes [b,c,e], Madalena M. Dias [b,c], Rosa Montes [f], Rosario Rodil [f], José Benito Quintana [f], Gabriel Antonio Cerrón-Calle [g,b,c], Sergi Garcia-Segura [g], Carlos J. Tavares [h], Vítor J.P. Vilar [b,c,*], Francisca C. Moreira [b,c,*]

[a] *Escola de Química e Alimentos, Universidade Federal do Rio Grande, Campus Santo Antônio da Patrulha, Rua Barão do Cahy 125,95500-000 Cidade Alta, Santo Antônio da Patrulha, RS, Brazil*

[b] *LSRE-LCM – Laboratory of Separation and Reaction Engineering - Laboratory of Catalysis and Materials, Faculty of Engineering, University of Porto, Rua Dr. Roberto Frias, 4200-465 Porto, Portugal*

[c] *ALiCE – Associate Laboratory in Chemical Engineering, Faculty of Engineering, University of Porto, Rua Dr. Roberto Frias, 4200-465 Porto, Portugal*

[d] *Instituto de Química, Universidade Federal do Rio Grande do Sul, Av. Bento Gonçalves 9500, 91501-970 Porto Alegre, RS, Brazil*

[e] *CoLAB NET4CO2, Rua Júlio de Matos, 828-882, 4200-355 Porto, Portugal*

[f] *Aquatic One Health Research Center (ARCUS) & Department of Analytical Chemistry, Nutrition and Food Chemistry, Universidade de Santiago de Compostela, R. Constantino Candeira, IIAA building, 15782Santiago de Compostela, Galicia, Spain.*

[g] *Nanosystems Engineering Research Center for Nanotechnology-Enabled Water Treatment, School of Sustainable Engineering and the Built Environment, Arizona State University, Tempe, AZ 85287-3005, USA*

[h] *CF-UM-UP – Centre of Physics of the Universities of Minho and Porto, University of Minho, 4804-533 Guimarães, Portugal*

[1] The first two authors contributed equally to this work.

[*]Corresponding authors:

Tel.: +351 918257824; E-mail: vilar@fe.up.pt (Vítor J.P. Vilar)

Tel.: +351 914332022; E-mail: francisca.moreira@fe.up.pt (Francisca C. Moreira)

2.1. Chemicals

4-methoxybenzyl alcohol (4-MBA, $C_8H_{10}O_2$) 98% purity (w/w) and *p*-anisaldehyde (PAA, $C_8H_8O_2$) 98% purity (w/w) supplied by Sigma-Aldrich were used in 4-MBA selective oxidation, cyclic voltammetry (CV), and as standard solutions for high-performance liquid chromatography (HPLC) calibration. Sodium sulfate anhydrous (Na_2SO_4) ≥99% purity (w/w) provided by Merck was used as the supporting electrolyte. Sodium hydroxide (NaOH) ≥99% purity (w/w) and sulfuric acid (H_2SO_4) 96% purity (w/w) supplied by Merck and PanReac, respectively, were used to prepare diluted solutions for pH adjustments during oxidation reactions, and the H_2SO_4 was also employed in total oxidants determination. 4-methoxybenzoic acid (4-MBZA, $C_8H_8O_3$), an oxidation by-product used as standard solutions for HPLC calibration, was 99% purity (w/w) from Sigma-Aldrich. Tert-butyl alcohol (TBA, $C_4H_{10}O$) 99.5% (w/w) and N,N´-dimethylthiourea (DMTU, $C_3H_8N_2S$) 99% purity (w/w) provided by Acros Organics, and methanol (MeOH, CH_4O) ≥99.8% purity (w/w) from Sigma-Aldrich were used as scavenger agents. Potassium iodide (KI) ≥99.5% purity (w/w) and sodium thiosulfate ($Na_2S_2O_3$) supplied by Merck were applied in total oxidants determination. Oxalic acid dihydrate ($C_2H_2O_4.2H_2O$) 99.5-102.5% purity (w/w) supplied by PanReac was used to prepare an eluent solution for the HPLC. Methanol (CH_4O) ≥99.8% purity (w/w) and acetonitrile (C_2H_3N) ≥99.9% purity (w/w), HiPerSolv CHROMANORM® eluents for HPLC, were supplied by VWR Chemicals. Ultrapure water was obtained from a Millipore® Direct-Q system (18.2 MΩ cm resistivity at 25 ºC). Demineralized water was obtained from a reverse osmosis system (Panice).

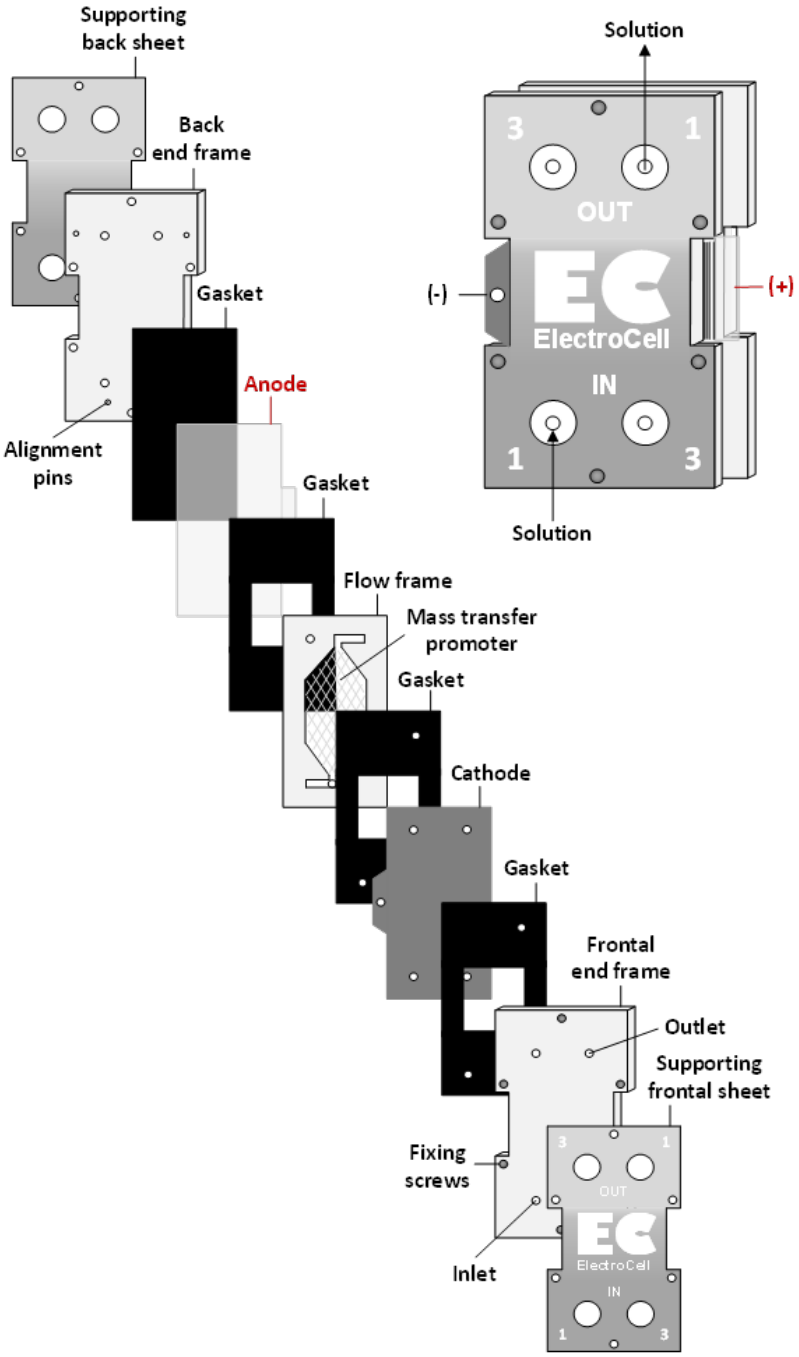

Figure SM-1. Sketches of the e^-Cell reactor (MicroFlowCell from ElectroCell, Denmark) disassembled (left) and assembled (right) equipped with the FTO anode (frontal views).

2.6. Analytical determinations - LC-QTOF-MS/MS analysis

The LC-QTOF-MS/MS analysis was carried out in an Agilent 1200 Series LC equipped with a degasser, a binary high-pressure pump, a LC column, an oven, and an autosampler. This LC system was coupled to an Agilent 6520 Series quadrupole time-of-flight (QTOF) mass spectrometry (MS) equipped with a dual electrospray ionization (Dual-ESI) source. The LC column was a Phenomenex® Synergi™ 4 µm Fusion-RP C18, 100 mm × 2 mm, at 35 °C. The mobile phase consisted of ultrapure water (eluent D) and methanol (eluent B), both containing 5 mM ammonium acetate. The gradient was as follows: 0-1 min, 0% B; 10 min, 100% B; 15 min, 100% B; 15-20 min, 0% B; 20 min, 0% B. The mobile phase flowed at 0.2 mL min^{-1}. For the QTOF, nitrogen was used as nebulizing and drying gas in electrospray ionization (ESI) and collision-induced dissociation (CID) gas in tandem mass spectrometry analysis (MS/MS). The ESI source operated in positive and negative polarities, and the parameters were as follows: gas temperature 350 ºC, drying gas 5 L min^{-1}, nebulizer 42 psig, capillary 4000 V, fragmentor 120 V, skimmer 65 V, and octapole RF 750 V. The instrument acquired MS spectra in centroid mode and operated at 2 GHz (extended-dynamic range), which provided a full width at half maximum (FWHM) resolution of ca. 4500 at m/z 121 and ca. 11,000 at m/z 922, scan range 50−1100 m/z. The manufacturer reference solution was also infused during every run and ionized with the second sprayer of the Dual-ESI at 5 psig. In this solution, masses, m/z 121.0509 and 922.0098 for ESI (+) and m/z 68.995758 and 1033.988109, were used for m/z-axis continuous recalibration. Instrument control and data treatment were done with different software included in the MassHunter package (Agilent Technologies). Briefly, the algorithm "Find by Molecular Feature" from the MassHunter Qualitative software was used to generate a list of features (chromatographic peaks and m/z values) with a response higher than 1000 counts. Data obtained were then analyzed with the software Mass Profiler Professional, which compares the intensity of those features at different reaction times, where features whose intensity increases as compared to time 0 can be possible reaction products. Then, formulas were generated for those features. The isotope pattern

matching, as well as the error between the experimental m/z values and those calculated (from the generated formula), is grouped by the software to provide a score in percentage, in which 100% would indicate a perfect match [1, 2]. The MS/MS analysis was finally obtained for the structure elucidation of the structures of the products, using CID with different collision energies between 10 and 40 V. PAA spectra were not available in any (open) library, and therefore its structure was assigned by evaluating its MS/MS spectra, as detailed in Figure SM-1 of Supplementary Material for a collision energy of 20 V (with the assigned fragment). The presence of 4-MBZA was confirmed as it matches the spectra stored at Massbank (record number KO000255). The acquired spectrum at 20 V is presented in Figure SM-2, which fits the record on Massbank m/z 109.10387, 92.0264, and 59.0139.

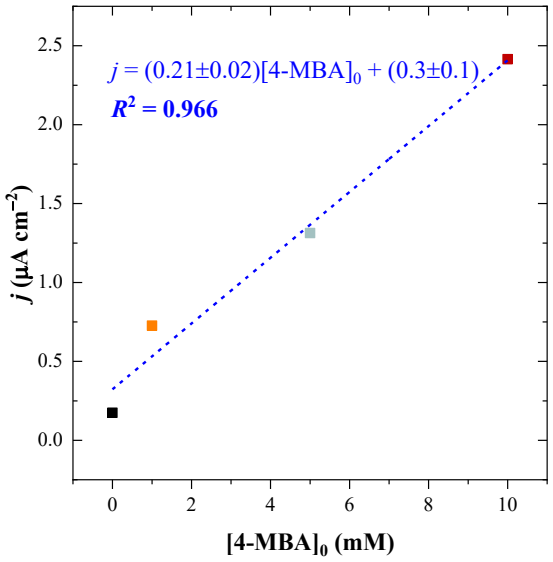

Figure SM-2. Linear relation between current density at 1.0 V *vs.* Ag/AgCl and 4-MBA concentration in CV curves for the bare FTO anode in a 100 mM Na_2SO_4 solution before and after adding different 4-MBA contents (T = 25±1 ºC).

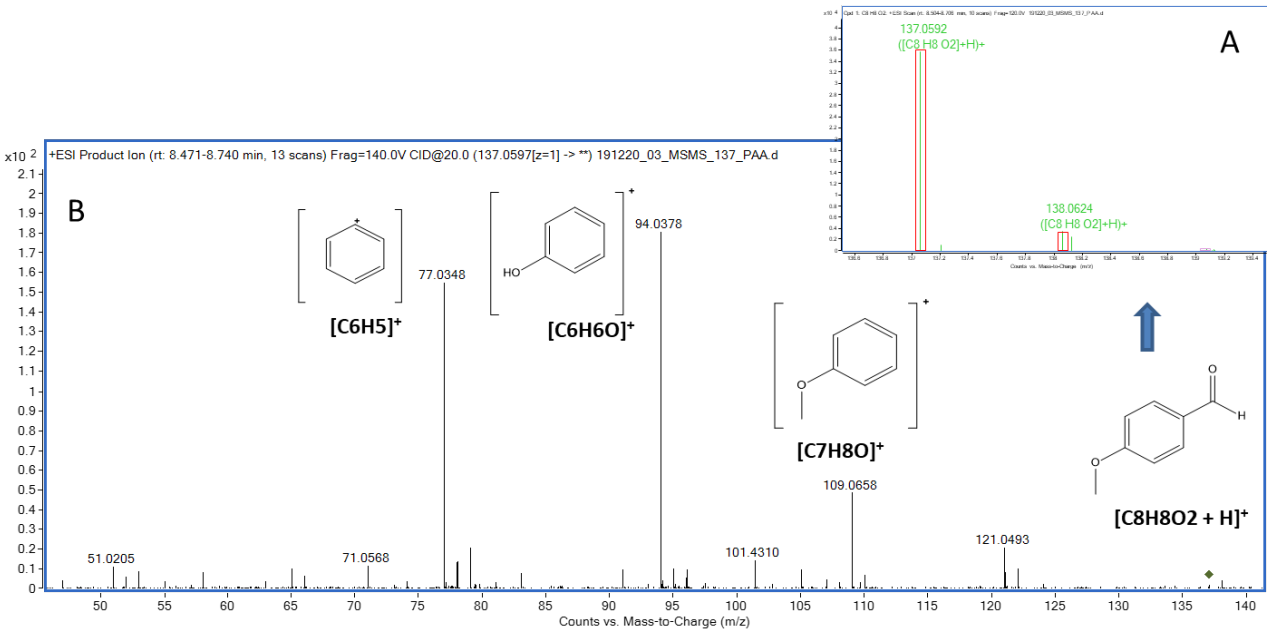

Figure SM-3. $[M+H]^+$ isotopic cluster (a) and MS/MS spectrum (b) interpretation for PAA (collision energy: 20V).

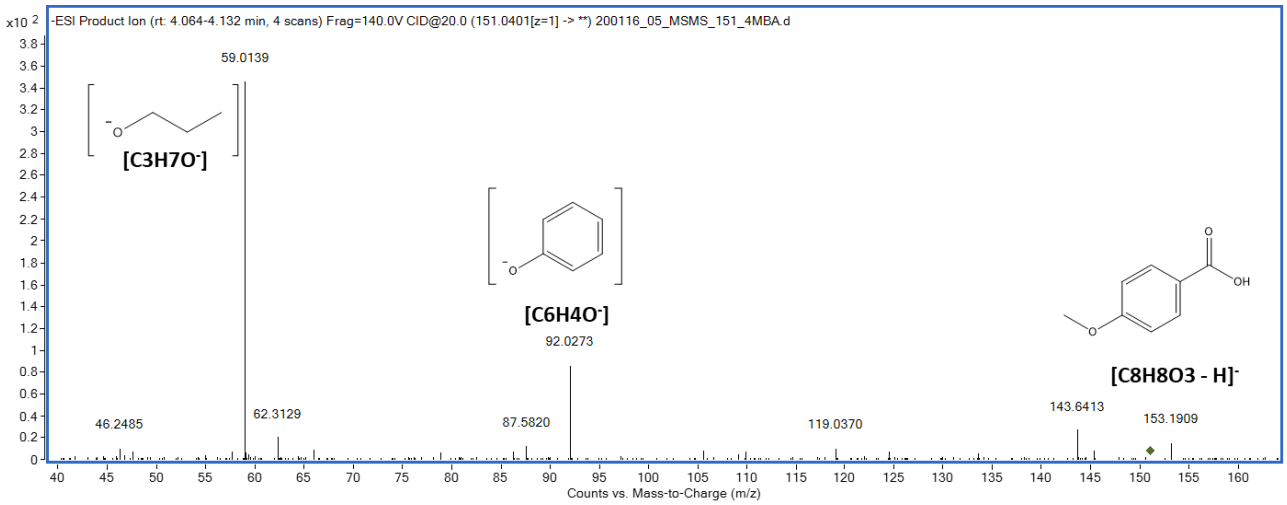

Figure SM-4. MS/MS spectrum and m/z peak assignment for 4-MBZA (collision energy: 20V), which was compared with Massbank record KO000255.

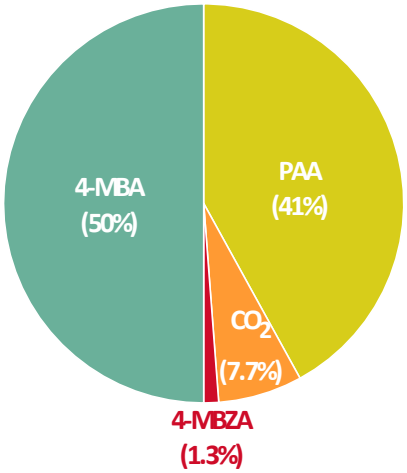

Figure SM-5. Carbon balance (% of C of each compound in solution) for 50% 4-MBA conversion in a typical 4-MBA selective oxidation to PAA in the e^-NETmix reactor. Conditions: j = 0.8 mA cm^{-2}, Re = 1750, [Na_2SO_4] = 50 mM, [4-MBA]$_0$ = 1.0 mM, T = 25±1 ºC, pH = 7.0±0.2.

Table SM-1. 4-MBA initial degradation rate ($r_{0,4\text{-MBA}}$) calculated by the pseudo-first-order kinetic model along with the corresponding residual variance (S^2_R) and coefficient of determination (R^2) for experiments in e^-NETmix.

e^-NETmix				
j **(mA cm^{-2})**	**Adjustment Δt (min)**	$r_{0,4\text{-MB}}$ **(× 10^{-3} mM min^{-1})**	S^2_R **(mM^2)**	R^2
0.3	0-60	7.8±0.2	9.7×10^{-4}	0.992
0.5	0-45	15.1±0.2	2.8×10^{-4}	0.998
0.8	0-20	27.8±0.9	1.1×10^{-3}	0.991
1.0	0-20	29.0±0.9	8.6×10^{-4}	0.994
1.5	0-20	31.1±0.7	5.3×10^{-4}	0.996
2.0	0-20	32.0±0.7	5.4×10^{-4}	0.997
3.0	0-20	32.1±0.9	7.9×10^{-4}	0.995
Re				
100	0-30	23±1	6.1×10^{-3}	0.970
190	0-20	29±2	3.4×10^{-3}	0.977
375	0-20	30±2	2.9×10^{-3}	0.980
500	0-20	29±1	1.3×10^{-3}	0.990
625	0-20	27±1	1.6×10^{-3}	0.987
1000	0-20	27±1	1.8×10^{-3}	0.985
1250	0-20	29±1	1.8×10^{-3}	0.987
1750	0-20	27.8±0.9	1.1×10^{-3}	0.991
[Na_2SO_4] (mM)				
0	0-30	17.8±0.5	7.9×10^{-4}	0.993
0.1	0-30	21.4±0.8	2.2×10^{-3}	0.987
1	0-30	28±1	2.2×10^{-3}	0.989
5	0-30	29.7±0.9	1.8×10^{-3}	0.993
10	0-30	27.6±0.7	1.2×10^{-3}	0.995
30	0-30	29±1	3.4×10^{-3}	0.986
50	0-20	27.8±0.9	1.1×10^{-3}	0.991
100	0-20	27±1	1.3×10^{-3}	0.990
[4-MBA]$_0$ (mM)				
0.25	0-20	12.0±0.6	2.4×10^{-4}	0.986
0.50	0-20	21.1±0.7	4.3×10^{-4}	0.992
1.0	0-20	27.8±0.9	1.1×10^{-3}	0.991
2.0	0-45	29.2±0.4	1.2×10^{-3}	0.998
3.0	0-60	28.8±0.8	1.6×10^{-2}	0.989

Table SM-2. 4-MBA initial degradation rate ($r_{0,4\text{-MBA}}$) calculated by the pseudo-first-order kinetic model along with the corresponding residual variance (S^2_R) and coefficient of determination (R^2) for experiments in e^-Cell.

e^-Cell				
j **(mA cm^{-2})**	**Adjustment Δt (min)**	$r_{0,4\text{-MBA}}$ **(× 10^{-3} mM min^{-1})**	S^2_R **(mM^2)**	R^2
0.3	0-60	7.0±0.3	4.8×10^{-3}	0.978
0.5	0-45	13.6±0.8	5.3×10^{-3}	0.970
0.8	0-30	17.9±0.5	8.0×10^{-4}	0.993
1.0	0-30	19.2±0.2	8.0×10^{-5}	0.999
1.5	0-30	19.7±0.4	5.4×10^{-4}	0.996
2.0	0-30	18.1±0.1	5.6×10^{-5}	0.999
3.0	0-30	18.9±0.4	5.9×10^{-4}	0.995
Re				
100	0-120	5.6±0.2	2.5×10^{-3}	0.991
190	0-90	8.6±0.1	7.6×10^{-4}	0.997
375	0-90	8.98±0.09	2.8×10^{-4}	0.999
500	0-60	9.8±0.6	7.9×10^{-3}	0.964
625	0-60	9.3±0.5	6.4×10^{-3}	0.967
1000	0-60	11.5±0.7	7.1×10^{-3}	0.972
1250	0-45	17.1±0.8	4.0×10^{-3}	0.983
1750	0-30	17.9±0.5	8.0×10^{-4}	0.993
[Na_2SO_4] (mM)				
0	0-45	13.3±0.4	1.8×10^{-3}	0.988
0.1	0-45	12.9±0.4	1.7×10^{-3}	0.988
1	0-45	14.1±0.5	2.6×10^{-3}	0.985
5	0-45	15.0±0.6	2.8×10^{-3}	0.985
10	0-45	15.8±0.5	1.9×10^{-3}	0.990
30	0-30	18.8±0.7	1.8×10^{-3}	0.986
50	0-30	17.9±0.5	8.0×10^{-4}	0.993
100	0-30	17.8±0.8	2.1×10^{-3}	0.982
[4-MBA]$_0$ (mM)				
0.25	0-30	6.1±0.2	8.8×10^{-5}	0.992
0.50	0-30	12.3±0.3	2.0×10^{-4}	0.996
1.0	0-30	17.9±0.5	8.0×10^{-4}	0.993
2.0	0-45	26.0±0.8	4.6×10^{-4}	0.999
3.0	0-60	26±1	4.6×10^{-2}	0.978

References

[1] I. Carpinteiro, R. Rodil, J.B. Quintana, R. Cela, Reaction of diazepam and related benzodiazepines with chlorine. Kinetics, transformation products and in-silico toxicological assessment, Water Res. 120 (2017) 280-289. https://doi.org/10.1016/j.watres.2017.04.063.

[2] B.J. Sieira, R. Rodil, R. Cela, J.B. Quintana, R. Montes, Transformation products of the high-volume production chemicals 1-vinyl-2-pyrrolidinone and 2-piperazin-1-ylethanamine formed by UV photolysis, Chemosphere 287 (2022) 132394. https://doi.org/10.1016/j.chemosphere.2021.132394.